










Computer-Aided Diagnosis Parameters of Invasive Carcinoma of No Special Type on 3T MRI: Correlation with Pathologic Immunohistochemical Markers

3T 자기공명영상에서 비특이 침윤성 유방암의 컴퓨터보조진단 인자들과 병리적 면역조직화학 표지자들과의 상관성

Jinho Jeong, MD¹ , Chang Suk Park, MD^{1*} , Jung Whee Lee, MD¹ ,
Kijun Kim, MD¹ , Hyeon Sook Kim, MD² ,
Sun-Young Jun, MD³ , Se-Jeong Oh, MD⁴ 

Departments of ¹Radiology, ³Pathology, and ⁴Surgery, Incheon St. Mary's Hospital, College of Medicine, The Catholic University of Korea, Incheon, Korea

²Department of Radiology, Eunpyeong St. Mary's Hospital, College of Medicine, The Catholic University of Korea, Seoul, Korea

Purpose To investigate the correlation between computer-aided diagnosis (CAD) parameters in 3-tesla (T) MRI and pathologic immunohistochemical (IHC) markers in invasive carcinoma of no special type (NST).

Materials and Methods A total of 94 female who were diagnosed with NST carcinoma and underwent 3T MRI using CAD, from January 2018 to April 2019, were included. The relationship between angiovolume, curve peak, and early and late profiles of dynamic enhancement from CAD with pathologic IHC markers and molecular subtypes were retrospectively investigated using Dwass, Steel, Critchlow-Fligner multiple comparison analysis, and univariate binary logistic regression analysis.

Results In NST carcinoma, a higher angiovolume was observed in tumors of higher nuclear and histologic grades and in lymph node (LN) (+), estrogen receptor (ER) (-), progesterone receptor (PR) (-), human epidermal growth factor 2 (HER2) (+), and Ki-67 (+) tumors. A high rate of delayed washout and a low rate of delayed persistence were observed in Ki-67 (+) tumors. In the binary logistic regression analysis of NST carcinoma, a high angiovolume was significantly associated with a high nuclear and histologic grade, LN (+), ER (-), PR (-), HER2 (+) status, and

Received April 14, 2021

Revised May 25, 2021

Accepted June 15, 2021

*Corresponding author

Chang Suk Park, MD
Department of Radiology,
Incheon St. Mary's Hospital,
College of Medicine,
The Catholic University of Korea,
56 Dongsu-ro, Bupyeong-gu,
Incheon 21431, Korea.

Tel 82-32-280-5183

Fax 82-32-280-5192

E-mail blounse@catholic.ac.kr

This is an Open Access article distributed under the terms of the Creative Commons Attribution Non-Commercial License (<https://creativecommons.org/licenses/by-nc/4.0>) which permits unrestricted non-commercial use, distribution, and reproduction in any medium, provided the original work is properly cited.

ORCID iDs

Jinho Jeong 
<https://orcid.org/0000-0001-8746-6820>
Chang Suk Park 
<https://orcid.org/0000-0002-0854-0111>
Jung Whee Lee 
<https://orcid.org/0000-0001-8949-5385>
Kijun Kim 
<https://orcid.org/0000-0003-3480-7489>
Hyeon Sook Kim 
<https://orcid.org/0000-0002-3699-3951>
Sun-Young Jun 
<https://orcid.org/0000-0002-3007-2094>
Se-Jeong Oh 
<https://orcid.org/0000-0002-2583-4218>

non-luminal subtypes. A high rate of washout and a low rate of persistence were also significantly correlated with the Ki-67 (+) status.

Conclusion Angiovolume and delayed washout/persistent rate from CAD parameters in contrast enhanced breast MRI correlated with predictive IHC markers. These results suggest that CAD parameters could be used as clinical prognostic, predictive factors.

Index terms Breast Neoplasms; Magnetic Resonance Imaging; Computer-Assisted Diagnosis; Immunohistochemistry

INTRODUCTION

Breast MRI has a high sensitivity of approximately 90% for breast cancer and is used as a complementary imaging modality to mammography and ultrasonography in the assessment of breast disease (1). Dynamic contrast-enhanced MRI (DCE-MRI) offers morphological and functional information, with outstanding sensitivity and variable specificity for breast cancer diagnosis (2-4). In addition, pharmacokinetic MRI parameters have been investigated for the differentiation of breast cancer subtypes (5). Recently, preoperative breast MRI has been highlighted not only as a diagnostic imaging method but also as a prognostic tool that can indicate different prognostic factors and surgical outcomes in invasive breast cancer (6, 7).

Computer-aided diagnosis (CAD) is widely used in breast MRI and provides improved sensitivity and specificity for readers with varying levels of experience by providing automated analysis of enhancement kinetics. By excluding lesions with a low threshold enhancement and reducing the interpretation time by automating the process, the false-positive rate for CAD is reduced by 25% at a 50% threshold and by 50% at a 100% threshold for enhancement compared with that for analysis performed by a radiologist (8).

Invasive breast cancer includes various histologic subtypes and they have a variety of unique morphological characteristics and MR enhancement patterns. Invasive carcinoma of no special type (NST) accounts for majority of breast cancers and has different clinical courses and prognoses according to pathologic immunohistochemical (IHC) markers. After the 2013 St. Gallen meeting, five subtypes (luminal A-like, luminal B-like human epidermal growth factor 2 [HER2] negative, luminal B-like HER2 positive, HER2 overexpression, and triple negative [TN]) were suggested, and the criteria of molecular subtypes was further specified (9). Contemporary treatment plans are increasingly guided by the molecular classification of breast cancer (10). To know the status of IHC markers and molecular subtypes preoperatively is helpful for deciding the treatment plan and predicting the patient prognosis. There were already a few studies which have investigated the correlation between CAD features and IHC markers, they have shown that CAD features could be used as prognostic markers (11-13). Differently from previous studies, we analyzed the invasive carcinoma of NST, the most common type of invasive breast cancer for excluding heterogeneity of subtypes.

The purpose of this study was to retrospectively investigate the correlation between CAD parameters in preoperative 3-tesla (3T) MRI with pathologic IHC markers in invasive carcinoma of NST.

MATERIALS AND METHODS

PATIENT POPULATION

The Institutional Review Board approved this study and required neither patient approval nor patient informed consent for the review of their images and records (IRB No. XC17RE-DI0052).

From January 2018 to April 2019, data from 450 patients who underwent breast MRI were examined. We excluded patients who underwent MRI examinations for benign breast diseases or chemotherapy evaluation and those who underwent MRI post-operation. Then, patients with specific types of invasive breast cancer such as invasive lobular carcinomas ($n = 2$), invasive cribriform carcinoma ($n = 1$), invasive medullary carcinoma ($n = 1$), invasive papillary carcinoma ($n = 1$) and invasive mucinous carcinoma ($n = 1$) were excluded for homogeneity of research. Consequently, 94 women (mean age, 58.84 years; range, 39–86 years) diagnosed with NST carcinoma who had undergone 3T breast MRI using the CAD system were retrospectively investigated. Surgical excision and pathologic study were performed in all patients.

DATA ACQUISITION AND ANALYSIS

MRI TECHNIQUE

All MRI examinations were performed using two 3T systems (MAGNETOM Skyra, Siemens Medical Solutions, Erlangen, Germany and Ingenia, Philips Medical Systems, Best, the Netherlands) with a dedicated array breast coil in the axial orientation. Patients were placed in the prone position.

MRI images from the Ingenia scanner used the following sequences: an axial, fat-suppressed, fast spin-echo T2-weighted imaging sequence (repetition time/echo time [TR/TE], 100032/70 ms; flip angle, 90°; 150 slices; field of view [FOV], 320 mm; matrix, 512 × 512; 1-mm slice thickness; no gap) and an axial diffusion-weighted sequence. Pre- and postcontrast dynamic axial T1-weighted three-dimensional, fat-suppressed, fat-spoiled gradient-echo sequences (TR/TE, 4.7/2.0 ms; flip angle, 12°; 1.0-mm slice thickness) were obtained before and at 76, 136, 196, 256, 316, 376, and 436 seconds after gadoterate meglumine injection.

MRI images from the MAGNETOM Skyra scanner were acquired using the following sequences: an axial, turbo spin-echo T2-weighted imaging sequence (TR/TE, 10190/76 ms; flip angle, 148°; 52 slices; FOV, 360 mm; matrix, 384 × 384; 2.5-mm slice thickness) and pre- and postcontrast axial T1-weighted fast low-angle shot three-dimensional, volumetric interpolated breath-hold examination sequences (TR/TE, 4.6/1.7 ms; flip angle, 10°; 0.9-mm slice thickness) obtained before and at 67, 127, 187, 247, and 367 seconds after gadoterate meglumine injection.

A bolus of 0.1 mmol/kg gadoterate meglumine (Dotarem; Guerbet, Villepinte, France) was intravenously injected by using an MRI-compatible power injector at a rate of 2 mL/s, followed immediately by a 20 mL saline flush.

CAD SYSTEM

The CAD system (CADstream, version 6.0; Confirma, Kirkland, WA, USA) received all T1-

weighted images, and breast tumors were automatically segmented into three dimensions. Then, CAD parameters such as angiovolume and tumor location were assessed for each lesion and retrospectively processed to generate kinetic parameters of dynamic contrast enhancement. The CAD systems compared pixel signal intensity values on the precontrast images and postcontrast series. A 50% threshold was set to balance the sensitivity and specificity (8, 14). If the pixel value was greater than the threshold, the pixel was shown in color, and a color overlay was rendered to the lesions meeting threshold enhancement criteria according to changes in the pixel values between the early contrast-enhanced and delayed contrast-enhanced series; the results were indicated as follows: persistent type (increased pixel signal intensity of greater than 10% from the early postcontrast series, color coded blue); washout type (decreased pixel signal intensity at the last postcontrast series greater than 10% from the early postcontrast series, color coded red); and plateau type (change in neither direction by more than 10%, color coded yellow). Thus, we used the following CAD parameters: curve peak (the highest pixel signal intensity in the early phase postcontrast series); angiovolume (the total volume of the enhancing lesion); early enhancement profiles (the rates of rapid [$> 100\%$] or medium [50%–100%] enhancing components within a tumor in the early phase postcontrast series); and delayed enhancement profiles (the rates of washout, plateau, and persistent types in the delayed phase postcontrast series) (Fig. 1A, B).

PATHOLOGIC IMMUNOHISTOCHEMICAL MARKERS

Pathologic IHC markers included nuclear and histologic grade, pathologic tumor size, vascular and lymphatic invasion status, and regional lymph node (LN), estrogen receptor (ER), progesterone receptor (PR), HER2, Ki-67, cytokeratin 5/6 (CK5/6) and epidermal growth factor receptor (EGFR) status. In our assessment, ER or PR (+) status was indicated by stained nuclei in $> 1\%$ of cancer cells in 10 high-power fields. The HER2 staining intensity was scored

Fig. 1. MR images with a computer-aided detection color overlay map in a 47-year-old female with histologic and nuclear grade 3, Ki-67 positive, estrogen receptor and/or progesterone receptor positive, luminal B subtype invasive carcinoma of no special type in the right breast.

A. Postcontrast T1-weighted image in the early phase shows an irregular and heterogeneously enhancing mass in the outer portion of the right breast.

B. Areas in red, yellow, and blue indicate washout delayed enhancement, plateau-delayed enhancement, and persistent delayed enhancement patterns, respectively. Kinetic curve shows a rapid early enhancement and a delayed washout-type curve. The initial peak enhancement value is 282%. With respect to the delayed-phase enhancement, 57% of the mass represents washout, 21% of the mass represents a persistent-type curve, and 21% represents a plateau-type curve.



as 0, 1+, 2+, or 3+. Tumors with scores of 3+ were classified as HER2 (+), whereas those with scores of 0 or 1+ were classified as HER2 (-). Tumors with scores of 2+ were further investigated with fluorescence *in situ* hybridization to determine the HER2 status. For the Ki-67 index status, we used a cutoff value of 15% for classification into negative and positive groups (15). For molecular subtype assessment, samples were classified into four groups according to hormone receptor status (ER and/or PR), HER2 status and Ki-67 index as follows: luminal A, hormone receptor (+), HER2 (-), and low levels of the Ki-67; luminal B, hormone receptor (+) and either HER2 (+) or HER2 (-) with high levels of Ki-67; TN, hormone receptor (-) and HER2 (-); and HER2-overexpression, hormone receptor (-) and HER2 (+). All values of pathologic IHC markers and pathologic tumor size were based on pathological reports from the electronic medical records of our institution.

STATISTICAL ANALYSIS

Dwass, Steel, Critchlow-Fligner multiple comparison analysis was used to compare the means of all pairs of CAD parameters and IHC markers with a nonparametric, pairwise comparison method. Spearman correlation analysis was used to assess correlations between CAD parameters and pathologic IHC markers. The Spearman correlation coefficient ranges from -1 to +1; +1 indicates a perfect positive association of ranks, zero indicates no association between ranks, and -1 indicates a perfect negative association of ranks.

Univariate binary logistic regression analysis was performed to study independent predictors by using dichotomized IHC markers as dependent variables and CAD parameters as covariates. Histologic and nuclear grades were grouped as low (grade I) or high (grade II or III). Molecular subtypes were classified as luminal (luminal A and luminal B) or nonluminal (HER2-overexpression and TN).

All data analyses were performed using SAS (version 9.4, SAS Institute Inc., Cary, NC, USA), and a *p* value below 0.05 was considered significant.

RESULTS

CAD parameters on 3T-MRI of invasive carcinoma of NST are summarized in Table 1.

CORRELATION BETWEEN CAD AND PATHOLOGIC AND IMMUNOHISTOCHEMICAL PARAMETERS

High mean angiovolume was related to ER (-), PR (-), and HER2 (+) status ($p = 0.002$, $p = 0.009$, $p = 0.004$, respectively). In addition, a higher mean angiovolume was observed in tumors of higher nuclear and histologic grade ($p = 0.001$ and $p < 0.001$, respectively) and in tumors of the LN (+), Ki-67 (+) and HER2-overexpression subtype ($p = 0.006$, $p = 0.035$, and $p = 0.006$, respectively). A high rate of washout and a low rate of persistent enhancement were observed in NST carcinoma with Ki-67 (+) ($p < 0.001$ and $p = 0.002$, respectively). The curve peak showed a tendency similar to that of angiovolume, but the correlation was not significant. Although a higher mean angiovolume was observed in CK5/6 (+) and EGFR (+) tumors, the correlations between these factors were not significant (Table 2). Angiovolume showed a moderate correlation with pathologic tumor size ($r = 0.632$, $p < 0.001$). The curve peak showed a weak

Table 1. CAD Parameters of Invasive Carcinoma, NST (NST Carcinoma)

MRI CAD Parameters	NST Carcinoma
Angiovolume	
Mean, SD	2.07 (2.59)
Min, max	0.02, 11.10
Curve pean	
Mean, SD	316.50 (179.40)
Min, max	78.00, 1151.00
Early rapid enhancement	
Mean, SD	82.69 (20.22)
Min, max	2.00, 100.00
Early medium enhancement	
Mean, SD	17.31 (20.22)
Min, max	0.00, 98.00
Delayed washout	
Mean, SD	25.71 (20.21)
Min, max	0.00, 90.00
Delayed plateau	
Mean, SD	22.18 (12.28)
Min, max	0.00, 66.00
Delayed persistent	
Mean, SD	52.15 (26.73)
Min, max	4.00, 100.00
Total	94

CAD = computer-aided diagnosis, max = maximum, min = minimum, NST = no special type, SD = standard deviation

correlation with pathologic tumor size (Table 3).

BINARY LOGISTIC REGRESSION ANALYSIS

High angiovolume was independently correlated with high nuclear grade (grade 2 and 3, odds ratio [OR] = 2.055, 95% confidence interval [CI]: 1.048–4.028, $p = 0.036$), high histologic grade (grade 2 and 3, OR = 2.175, 95% CI: 1.152–4.107, $p = 0.017$) and LN (+) status (OR = 0.802, 95% CI: 0.668–0.963, $p = 0.018$) in invasive carcinoma of NST (Table 4). Additionally, high angiovolume correlated with ER (-) (OR = 1.287, 95% CI: 1.077–1.538, $p = 0.006$), PR (-) (OR = 1.214, 95% CI: 1.025–1.439, $p = 0.025$), and HER2 (+) status (OR = 0.755, 95% CI: 0.616–0.926, $p = 0.007$) (Fig. 2A, B). A higher washout rate of NST carcinoma correlated with Ki-67 (+) status (OR = 0.966, 95% CI: 0.944–0.989, $p = 0.004$). Although a high angiovolume correlated with Ki-67 (+) status, this correlation was not significant (OR = 0.844, 95% CI: 0.704–1.013, $p = 0.069$).

DISCUSSION

Our study may suggest that a high angiovolume on CAD is associated with not only pathology size but also high nuclear and histologic grade; LN (+), ER (-), PR (-), and HER2 (+) status;

Table 2. IHC Markers and CAD Parameters of NST Carcinoma

IHC Markers	Angiovolume (cc)	Curve Peak (%)	Early Component (%)		Delayed Component (%)		
			Rapid	Medium	Washout	Plateau	Persistent
Nuclear grade							
1	0.65 ± 0.93*	234.38 ± 93.62	77.00 ± 27.80	23.00 ± 27.80	20.36 ± 17.97	22.25 ± 14.89	57.50 ± 31.44
2	2.25 ± 2.79 [†]	330.80 ± 195.28	84.80 ± 16.98	15.20 ± 16.98	25.54 ± 19.52	22.09 ± 11.83	52.40 ± 25.69
3	2.66 ± 2.68 [†]	337.36 ± 178.58	80.77 ± 21.51	19.23 ± 21.51	30.83 ± 23.11	21.68 ± 11.79	47.50 ± 26.75
<i>p</i>	0.001	0.088	0.839	0.839	0.366	0.977	0.569
Histologic grade							
1	0.63 ± 0.83*	270.65 ± 160.26	75.90 ± 27.61	24.10 ± 27.61	21.69 ± 17.21	22.20 ± 13.87	56.20 ± 29.67
2	2.24 ± 2.79 [†]	318.92 ± 191.14	84.62 ± 17.63	15.38 ± 17.63	24.82 ± 20.09	21.38 ± 11.69	53.84 ± 26.20
3	2.96 ± 2.78 [†]	348.13 ± 171.30	83.65 ± 17.66	16.35 ± 17.66	31.91 ± 22.37	23.26 ± 12.44	44.83 ± 25.55
<i>p</i>	<0.001	0.133			0.288	0.796	0.315
Lymphatic invasion							
Positive	2.68 ± 2.83	303.58 ± 117.99	86.96 ± 16.45	13.04 ± 16.45	26.04 ± 19.08	24.71 ± 11.62	49.29 ± 26.02
Negative	1.85 ± 2.50	320.91 ± 196.64	81.23 ± 21.27	18.77 ± 21.27	25.59 ± 20.71	21.31 ± 12.47	53.13 ± 27.08
<i>p</i>	0.090	0.683			0.828	0.178	0.471
Venous invasion							
Positive	3.75 ± 3.16	354.25 ± 141.99	90.25 ± 8.22	9.75 ± 8.22	23.00 ± 18.85	20.00 ± 10.80	56.50 ± 29.83
Negative	1.99 ± 2.58	315.81 ± 182.14	82.18 ± 20.59	17.82 ± 20.59	25.85 ± 20.47	22.18 ± 12.42	52.03 ± 26.89
<i>p</i>	0.251	0.363	0.848	0.848	0.711	0.730	0.733
Lymph node							
Positive	3.05 ± 2.77	325.92 ± 106.56	89.56 ± 12.24	10.44 ± 12.24	28.64 ± 20.03	25.04 ± 11.33	46.40 ± 25.94
Negative	1.59 ± 2.24	313.06 ± 199.70	81.36 ± 20.98	18.64 ± 20.98	24.75 ± 20.28	21.37 ± 12.46	53.90 ± 26.59
<i>p</i>	0.006	0.063	0.158	0.158	0.329	0.140	0.246
ER status							
Positive	1.63 ± 2.18	309.79 ± 183.12	82.36 ± 20.54	17.64 ± 20.54	26.39 ± 21.05	22.53 ± 12.66	51.10 ± 27.83
Negative	3.58 ± 3.33	339.76 ± 168.03	83.86 ± 19.51	16.14 ± 19.51	23.35 ± 17.21	20.95 ± 11.08	55.81 ± 22.72
<i>p</i>	0.002	0.243	0.820	0.820	0.730	0.400	0.434
PR status							
Positive	1.61 ± 2.26	317.00 ± 195.25	82.74 ± 20.98	17.26 ± 20.98	26.50 ± 21.90	22.55 ± 13.11	50.97 ± 28.54
Negative	2.94 ± 3.00	315.50 ± 146.82	82.59 ± 18.97	17.41 ± 18.97	24.17 ± 16.66	21.47 ± 10.66	54.44 ± 23.08
<i>p</i>	0.009	0.518	0.803	0.803	0.848	0.609	0.470
HER2 status							
Positive	4.42 ± 3.68	409.10 ± 214.49	74.80 ± 25.88	25.20 ± 25.88	22.73 ± 18.27	20.40 ± 11.68	56.70 ± 24.45
Negative	1.79 ± 2.31	305.46 ± 172.98	83.63 ± 19.42	16.37 ± 19.42	26.06 ± 20.50	22.39 ± 12.40	51.61 ± 27.07
<i>p</i>	0.004	0.071	0.308	0.308	0.708	0.754	0.511
Ki-67 status							
Positive	2.55 ± 2.85	323.68 ± 178.60	85.72 ± 15.65	14.28 ± 15.65	31.72 ± 18.47	24.54 ± 10.37	43.78 ± 22.15
Negative	1.53 ± 2.19	313.02 ± 181.49	80.56 ± 22.78	19.44 ± 22.78	19.31 ± 20.14	19.93 ± 13.65	60.79 ± 28.24
<i>p</i>	0.035	0.537	0.445	0.445	<0.001	0.052	0.002
CK5/6 status							
Positive	2.57 ± 2.69	299.76 ± 95.63	85.82 ± 14.25	14.18 ± 14.25	24.82 ± 18.72	20.76 ± 10.40	54.59 ± 24.05
Negative	1.95 ± 2.59	321.42 ± 194.34	81.79 ± 21.39	18.21 ± 21.39	25.93 ± 20.77	22.38 ± 12.75	51.70 ± 27.57
<i>p</i>	0.139	0.672	0.726	0.726	0.920	0.406	0.709

Table 2. IHC Markers and CAD Parameters of NST Carcinoma (Continued)

IHC Markers	Angiovolume (cc)	Curve Peak (%)	Early Component (%)		Delayed Component (%)		
			Rapid	Medium	Washout	Plateau	Persistent
EGFR status							
Positive	2.61 ± 3.02	320.81 ± 113.57	88.38 ± 13.52	11.63 ± 13.52	28.81 ± 17.72	23.31 ± 11.85	47.88 ± 23.48
Negative	1.95 ± 2.52	316.77 ± 191.66	81.31 ± 21.27	18.69 ± 21.27	25.08 ± 20.86	21.83 ± 12.47	53.13 ± 27.57
<i>p</i>	0.544	0.336	0.255	0.255	0.348	0.818	0.527
Subtypes							
LA	1.42 ± 2.07*	302.44 ± 173.44	80.90 ± 22.07	19.10 ± 22.07	21.96 ± 19.98	22.10 ± 13.73	55.94 ± 28.65
LB	2.09 ± 2.40*†	325.78 ± 205.79	85.52 ± 16.73	14.48 ± 16.73	36.00 ± 20.49	23.48 ± 10.14	40.57 ± 23.16
HER2	5.80 ± 4.44†	476.60 ± 269.28	72.20 ± 31.32	27.80 ± 31.32	21.46 ± 17.13	19.40 ± 13.32	59.00 ± 24.48
TN	2.88 ± 2.71†	297.00 ± 100.60	87.50 ± 13.66	12.50 ± 13.66	23.94 ± 17.75	21.44 ± 10.75	54.81 ± 22.89
<i>p</i>	0.006	0.291	0.669	0.669	0.053	0.825	0.135

*† Different letters indicate significant differences between groups based on the Dwass, Steel, Critchlow-Fligner multiple comparison analysis. CAD = computer-aided diagnosis, EGFR = epidermal growth factor receptor, ER = estrogen receptor, HER2 = human epidermal growth factor 2, IHC = immunohistochemistry, LA = luminal A, LB = luminal B, NST = no special type, PR = progesterone receptor, TN = triple negative

Table 3. Spearman Correlation between Pathology Size and Computer-Aided Diagnosis Parameters of NST Carcinoma

Pathology Size	Angiovolume	Curve Peak	Early Component		Delayed Component		
			Rapid	Medium	Washout	Plateau	Persistent
NST carcinoma	0.632	0.321	-0.004	0.004	0.106	-0.009	-0.035
<i>p</i>	<0.001	0.001	0.972	0.972	0.308	0.934	0.734

NST = no special type

and nonluminal subtypes in NST carcinoma. A high rate of washout and a low rate of persistent enhancement on CAD correlated with Ki-67 (+) status, too.

Angiogenesis, the rapid increase in the formation of blood vessels, is required for the supply of sufficient oxygen and nutrition for breast tumor growth, and breast cancer cells require persistent nourishment and oxygen supply through the vascular network of capillaries in the system (16). It has been documented that tumor angiogenesis is a critical factor in breast tumor growth and aggressiveness, and contrast enhancement is thought to reflect tumor angiogenesis (17). Therefore, an increased level of angiogenesis is associated with decreased survival in breast cancer patients (18). The CAD program reconstructs the enhancing component within a tumor meeting a given threshold and can be used to calculate the volume of this component, which is referred to as angiovolume. We hypothesized that this value can indirectly represent tumor angiogenesis. Consequently, we suggest that angiovolume on CAD could provide vital prognostic information in breast cancer patients. Angiovolume is already known to correlate with the response to neoadjuvant chemotherapy and the survival rate (6). In addition, angiovolume may be related to pathologic tumor size and high Ki-67 expression (12). In our demonstration, a higher mean angiovolume was observed in Ki-67 (+) NST carcinoma than Ki-67 (-) NST carcinoma. However, this difference was not significant in the binary logistic regression analysis. We also found that high angiovolume correlated with not only pathologic tumor size but also high nuclear and histologic grade; LN (+), ER (-), PR (-),

Table 4. Results of the Univariate Binary Logistic Regression Analysis between Immunohistochemistry Markers and Computer-Aided Diagnosis Parameters

	NST Carcinoma	
	Odds Ratio (95% CI)	p-Value
Nuclear grade 2*		
Angiovolume	2.055 (1.048, 4.028)	0.036
Histologic grade 2 [†]		
Angiovolume	2.175 (1.152, 4.107)	0.017
LN		
Curve peak	0.999 (0.997, 1.002)	0.510
Angiovolume	0.802 (0.668, 0.963)	0.018
ER status		
Angiovolume	1.287 (1.077, 1.538)	0.006
PR status		
Angiovolume	1.214 (1.025, 1.439)	0.025
HER2 status		
Angiovolume	0.755 (0.616, 0.926)	0.007
Ki-67		
Washout	0.966 (0.944, 0.989)	0.004
Persistent	1.027 (1.009, 1.045)	0.003
Angiovolume	0.844 (0.704, 1.013)	0.069
CK5/6		
Angiovolume	0.872 (0.755, 1.008)	0.063
Subtype [‡]		
Angiovolume	0.777 (0.650, 0.929)	0.006

*Nuclear grade was grouped into 1 and 2 + 3.

[†]Histologic grade was grouped into 1 and 2 + 3.

[‡]Subtype was grouped into luminal (luminal A and B subtypes) and nonluminal (HER2 overexpression and triple negative subtypes).

CI = confidence interval, ER = estrogen receptor, HER2 = human epidermal growth factor 2, LN = lymph node, NST = no special type, PR = progesterone receptor

and HER2 (+) status; and nonluminal subtypes. According to Bharti et al. (19), the mean microvessel density on pathologic specimens was the highest in ER (-) and PR (-) samples, and a significant correlation was found between ER status and mean vascular density. Song et al. (20) reported that circumscribed mass margin, associated nonmass enhancement on MR images, high histologic grade, high Ki-67 index, and older age could be associated with HER2 positivity.

The curve peak is the highest enhancing pixel in the early phase of enhancement on dynamic enhancement images. Although the curve peak shows a similar tendency to angiovolume in our study, the correlation between the two parameters was not significant.

For the time-signal intensity curve (TIC) pattern, early rapid enhancement with delayed washout is generally regarded as a suspicious pattern in the area of greatest enhancement in a manually drawn region of interest within a tumor on breast MRI. Few studies have investigated the correlation of the TIC and the molecular subtypes of breast cancer. A study reported

Fig. 2. MR images with a computer-aided detection color overlay map in a 61-year-old female with high angiovolume (6.1 cc) and non-luminal subtype (HER2-overexpression subtype; estrogen receptor-negative, progesterone receptor-negative, HER2-positive and Ki-67-positive) invasive carcinoma of no special type in the left breast, showing histologic and nuclear grade 3. Regional lymph node was metastasis-positive.

A. Postcontrast T1-weighted image in the early phase shows an irregular and heterogeneously enhancing mass in the upper inner quadrant of the left breast.

B. Kinetic curve graph shows a rapid early enhancement and a delayed washout-type curve. The initial peak enhancement value is 521%. With respect to the delayed-phase enhancement, 25% of the mass represents washout, 57% of the mass represents a persistent-type curve, and 17% represents a plateau-type curve.

HER2 = human epidermal growth factor 2



that the TN breast cancer subtype was significantly associated with high histologic grade and a persistent enhancement pattern on breast MRI. This difference in the TIC pattern between the TN breast cancer subtype and other breast cancer subtypes may be due to the heterogeneity of the internal enhancement of TN breast cancer subtype (21). Our study automatically obtained the TIC and the rates of early and delayed enhancement profiles from the whole lesion by CAD instead of a single TIC pattern. We did not identify significant differences in the rates of persistent or washout patterns between subtypes.

Ki-67 is a nuclear protein associated with cellular proliferation and a powerful prognostic marker in breast cancer. It is helpful in assessing the risk of recurrence for luminal subtype breast cancers (22). Song et al. (12) reported that kinetic features such as peak enhancement, angiovolume, and a delayed plateau pattern showed positive correlations with the Ki-67 index. Tumors that proliferate faster show faster enhancement on DCE-MRI (23). Another study found that a washout curve may predict a higher Ki-67 index (24). Our study also revealed that a high rate of delayed washout and a low rate of delayed persistent enhancement in NST carcinoma correlated with Ki-67 (+) status, as in previous studies.

CK5/6 and EGFR are adverse prognostic markers in TN breast cancer (25). While cancers positive for these markers showed a higher mean angiovolume than those negative for these markers, the correlation was not significant in this study.

Invasive cancers are known to present rapid enhancement kinetic curves. Nam et al. (26) suggested that higher histologic grade and ER (-), PR (-) and p53 (+) status are associated with a higher rate of rapid enhancement components on early phase enhancement. However, in our study, early enhancement profiles showed no significant association with any IHC markers.

Our study has some limitations. First, there were relatively small numbers of HER2-overexpression cases ($n = 15$) compared with the sample sizes of the other groups. Second, our

study was performed retrospectively in a single center. These results should be supported in larger group studies and prospective studies. Moreover, morphologic characteristics of the lesion according to standardized Breast Imaging-Reporting and Data System descriptors were not considered. Combining CAD parameters with descriptors such as spiculated or irregular margins and shape strongly indicating malignancy could lead to closer correlations of these features with IHC markers, and these results could finally suggest a more precise clinical course. Further comparison studies of each CAD feature and IHC markers of cancer may help explain these correlations.

In conclusion, our results suggest that the angiovolume and delayed washout/persistent rate from CAD parameters of invasive carcinoma of NST are the most useful predictive factor reflecting IHC markers of breast cancer preoperatively.

Author Contributions

Conceptualization, P.C.S.; data curation, P.C.S., J.J.; formal analysis, P.C.S., K.H.S.; investigation, P.C.S., J.J., J.S., O.S.; methodology, P.C.S., K.K.; project administration, P.C.S.; resources, P.C.S., J.S., O.S.; software, J.J., L.J.W.; supervision, P.C.S., K.H.S.; validation, L.J.W., K.K.; visualization, K.H.S.; writing—original draft, J.J.; and writing—review & editing, P.C.S., K.H.S.

Conflicts of Interest

The authors have no potential conflicts of interest to disclose.

Funding

None

Acknowledgments

Statistical evaluation was supported by the Department of Biostatistics of the Catholic Research Coordinating Center.

REFERENCES

1. Peters NH, Borel Rinkes IH, Zuithoff NP, Mali WP, Moons KG, Peeters PH. Meta-analysis of MR imaging in the diagnosis of breast lesions. *Radiology* 2008;246:116-124
2. Morris EA. Diagnostic breast MR imaging: current status and future directions. *Radiol Clin North Am* 2007; 45:863-880, vii
3. Morrow M, Waters J, Morris E. MRI for breast cancer screening, diagnosis, and treatment. *Lancet* 2011;378: 1804-1811
4. Pinker-Domenig K, Bogner W, Gruber S, Bickel H, Duffy S, Scherthaner M, et al. High resolution MRI of the breast at 3 T: which BI-RADS® descriptors are most strongly associated with the diagnosis of breast cancer? *Eur Radiol* 2012;22:322-330
5. Leithner D, Wengert GJ, Helbich TH, Thakur S, Ochoa-Albiztegui RE, Morris EA, et al. Clinical role of breast MRI now and going forward. *Clin Radiol* 2018;73:700-714
6. Kim JJ, Kim JY, Kang HJ, Shin JK, Kang T, Lee SW, et al. Computer-aided diagnosis-generated kinetic features of breast cancer at preoperative MR imaging: association with disease-free survival of patients with primary operable invasive breast cancer. *Radiology* 2017;284:45-54
7. Koh J, Park AY, Ko KH, Jung HK. Can enhancement types on preoperative MRI reflect prognostic factors and surgical outcomes in invasive breast cancer? *Eur Radiol* 2019;29:7000-7008
8. Lehman CD, Peacock S, DeMartini WB, Chen X. A new automated software system to evaluate breast MR examinations: improved specificity without decreased sensitivity. *AJR Am J Roentgenol* 2006;187:51-56
9. Goldhirsch A, Winer EP, Coates AS, Gelber RD, Piccart-Gebhart M, Thürlimann B, et al. Personalizing the treatment of women with early breast cancer: highlights of the St Gallen International Expert Consensus on the Primary Therapy of Early Breast Cancer 2013. *Ann Oncol* 2013;24:2206-2223

10. Weigelt B, Horlings HM, Kreike B, Hayes MM, Hauptmann M, Wessels LF, et al. Refinement of breast cancer classification by molecular characterization of histological special types. *J Pathol* 2008;216:141-150
11. Baltzer PA, Vag T, Dietzel M, Beger S, Freiberg C, Gajda M, et al. Computer-aided interpretation of dynamic magnetic resonance imaging reflects histopathology of invasive breast cancer. *Eur Radiol* 2010;20:1563-1571
12. Song SE, Cho KR, Seo BK, Woo OH, Jung SP, Sung DJ. Kinetic features of invasive breast cancers on computer-aided diagnosis using 3T MRI data: correlation with clinical and pathologic prognostic factors. *Korean J Radiol* 2019;20:411-421
13. Yamaguchi K, Abe H, Newstead GM, Egashira R, Nakazono T, Imaizumi T, et al. Intratumoral heterogeneity of the distribution of kinetic parameters in breast cancer: comparison based on the molecular subtypes of invasive breast cancer. *Breast Cancer* 2015;22:496-502
14. Levman JE, Causer P, Warner E, Martel AL. Effect of the enhancement threshold on the computer-aided detection of breast cancer using MRI. *Acad Radiol* 2009;16:1064-1069
15. Soliman NA, Yussif SM. Ki-67 as a prognostic marker according to breast cancer molecular subtype. *Cancer Biol Med* 2016;13:496-504
16. Castañeda-Gill JM, Vishwanatha JK. Antiangiogenic mechanisms and factors in breast cancer treatment. *J Carcinog* 2016;15:1
17. Weidner N, Folkman J, Pozza F, Bevilacqua P, Allred EN, Moore DH, et al. Tumor angiogenesis: a new significant and independent prognostic indicator in early-stage breast carcinoma. *J Natl Cancer Inst* 1992;84:1875-1887
18. Madu CO, Wang S, Madu CO, Lu Y. Angiogenesis in breast cancer progression, diagnosis, and treatment. *J Cancer* 2020;11:4474-4494
19. Bharti JN, Rani P, Kamal V, Agarwal PN. Angiogenesis in breast cancer and its correlation with estrogen, progesterone receptors and other prognostic factors. *J Clin Diagn Res* 2015;9:EC05-EC07
20. Song SE, Bae MS, Chang JM, Cho N, Ryu HS, Moon WK. MR and mammographic imaging features of HER2-positive breast cancers according to hormone receptor status: a retrospective comparative study. *Acta Radiol* 2017;58:792-799
21. Uematsu T. MR imaging of triple-negative breast cancer. *Breast Cancer* 2011;18:161-164
22. Arima N, Nishimura R, Osako T, Okumura Y, Nakano M, Fujisue M, et al. Ki-67 index value and progesterone receptor status can predict prognosis and suitable treatment in node-negative breast cancer patients with estrogen receptor-positive and HER2-negative tumors. *Oncol Lett* 2019;17:616-622
23. Caiazzo C, Di Micco R, Esposito E, Sollazzo V, Cervotti M, Varelli C, et al. The role of MRI in predicting Ki-67 in breast cancer: preliminary results from a prospective study. *Tumori* 2018;104:438-443
24. Lee SH, Cho N, Kim SJ, Cha JH, Cho KS, Ko ES, et al. Correlation between high resolution dynamic MR features and prognostic factors in breast cancer. *Korean J Radiol* 2008;9:10-18
25. Abdelrahman AE, Rashed HE, Abdelgawad M, Abdelhamid MI. Prognostic impact of EGFR and cytokeratin 5/6 immunohistochemical expression in triple-negative breast cancer. *Ann Diagn Pathol* 2017;28:43-53
26. Nam SY, Ko ES, Lim Y, Han BK, Ko EY, Choi JS, et al. Preoperative dynamic breast magnetic resonance imaging kinetic features using computer-aided diagnosis: association with survival outcome and tumor aggressiveness in patients with invasive breast cancer. *PLoS One* 2018;13:e0195756

3T 자기공명영상에서 비특이 침윤성 유방암의 컴퓨터보조진단 인자들과 병리적 면역조직화학 표지자들과의 상관성

정진호¹ · 박창숙^{1*} · 이정휘¹ · 김기준¹ · 김현숙² · 전선영³ · 오세정⁴

목적 3-tesla (이하 T) 자기공명영상에서 비특이 침윤성 유방암의 컴퓨터보조진단 인자들과 병리적 면역조직화학 표지자들과의 상관성을 알아보고자 하였다.

대상과 방법 2018년 1월부터 2019년 4월까지 비특이 침윤성 유방암으로 진단받은 총 94명의 3T 자기공명영상에서 컴퓨터보조진단 시스템을 통해 얻은 혈관조영부피, 최대 조영증강, 조영기 및 지연 조영증강 양상과 면역화학인자와 유방암의 분자형 아형과의 상관성을 Dwass, Steel, Critchlow-Fligner 비교 분석과 이분형 로지스틱 회귀 분석을 이용하여 후향적으로 연구하였다.

결과 혈관조영부피가 큰 비특이 침윤성 유방암이 핵등급과 조직학적 등급이 높고, 림프절 전이가 있고, 에스트로겐 수용체/프로게스테론 수용체 음성, 인간 표피성장인자수용체 2/Ki-67 양성인 비특이 침윤성 유방암에서 지연기 소실 성분 비율이 높고 지연기 지속 조영증강 비율이 낮았다. 이항회귀분석에서는 컴퓨터보조진단 시스템의 요소 중 혈관조영부피 인자가 독립적으로 핵등급, 조직학적 등급, 림프절 전이, 에스트로겐/프로게스테론 수용체, 인간 표피성장인자수용체 2와 Ki-67과 상관성이 있고, 지연기 소실 및 지속 조영증강 인자가 Ki-67과 상관성이 있었다.

결론 조영증강 유방 MRI 컴퓨터보조진단 시스템 인자 중 혈관조영부피 요소와 지연기 소실/지속 조영증강 비율이 예후 예측 인자로 알려진 면역화학인자들과 연관성이 높아 임상적 예후 예측 인자로서 이용될 수 있을 것으로 사료된다.

가톨릭대학교 의과대학 인천성모병원 ¹영상의학과, ³병리과, ⁴외과,
²가톨릭대학교 의과대학 은평성모병원 영상의학과